STRUCTURAL ANALYSIS OF MODERATELY-THICK FIBER-STEERED COMPOSITE CONICAL PANELS

Yazdani Sarvestani, H.[1], Akbarzadeh, A.H.*[1], Hojjat, M.[2]
[1]AM^{3}L Laboratory, Department of Bioresource Engineering, McGill University, Island of Montreal, QC, Canada H9X 3V9
[2]Department of Mechanical and Industrial Engineering, Concordia University, Montreal, QC, Canada H3G 1M8
* Corresponding author (hamid.akbarzadeh@mcgill.ca)
Keywords: *Automated fiber placement; Moderately-thick fiber-steered composite cylinder; Elasticity displacement field.*

ABSTRACT

One of the recently developed methods of composite manufacturing is robot-assisted manufacturing; so-called Automated Fiber Placement (AFP). Through fiber steering along optimal curvilinear paths, AFP enables tailoring the material stiffness within laminated composite structures. This type of laminated composites is known as variable stiffness (VS) laminates which can improve the structural performance of composite structures. Recently, the use of AFP has been extended to design and manufacture of moderately-thick composites, especially for applications in manned submersibles and wind turbine blades. This paper focuses on a structural analysis of moderately-thick fiber-steered composite conical panels using Layer-wise method. The principle of minimum total potential energy and state-space approaches are applied to obtain buckling loads, natural frequencies, and bending stresses within the VS composite conical panels. Neglecting the manufacturing defects, several examples for buckling loads, natural frequencies and bending stress distributions in VS conical panels are studied.

1 INTRODUCTION

Over the past few decades, laminated composite structures have been extensively used in a wide range of applications from aerospace and automotive to naval, as well as in construction because of their high specific stiffness and strength properties and capability. Composite laminates are commonly manufactured by stacking the layers of dissimilar fiber orientations, or material constituents [1]. This conventional method of composite manufacturing is being replaced by advanced fabrication technologies, e.g. Automated Fiber Placement (AFP) and Additive Manufacturing. The advantages of AFP technology include, but are not limited to, improved quality, reduced waste material, reduced labour costs, accuracy and repeatability of the production process, and reduced manufacturing time [2]. Another benefit of AFP technology is its ability to steer fibres on the plane of a ply to fabricate controlled curvilinear paths, a process that was initially developed in [3]. This capability provides designers with the ability to tailor the structural behavior of composites' parts not only through the thickness to change the stiffness and strength properties (straight fiber composites design) but also by spatially varying the point wise fiber orientations by actively steering individual fibre tows.

In the literature, most of researchers have used two main approaches, finite element modeling or equivalent single-layer (ESL) theories, to obtain and optimize structural and thermal responses of fiber-steered (i.e., VS) composite structures subjected to multiple load scenarios, as discussed in the review paper [4]. Cylindrical and conical panels are also widely used in aerospace applications such as centre and aft fuselages. The numerical investigations on VS cylindrical and conical structures include but are not limited to bending-induced buckling analysis [5, 6], axial buckling analysis [7, 8], vibration response [9, 10], thermal behavior [11, 12], postbuckling simulation [13, 14], and multi-objective design [15, 16]. The second approach, ESL theories such as classical lamination and first and third order shear deformation theories (CLT, FSDT, and TSDT), has also been employed for structural analysis of fiber-steered composite laminates for flat panels in [17, 18], cylinders in [19], and conical panels in [20]. In this study, Layer-wise theory is of interest. In it, each physical layer can be modeled as a finite number of numerical and independent layers [21, 22]. Furthermore, research studies by [23, 24] show that Layer-wise theory is computationally less expensive as compared to finite element simulations. Although a few investigations have used this kind of theory for a deflection response [25], free vibration [26] of fiber-steered plates, and static analysis of doubly-curved fiber-steered panels [27], less attention has been paid to fully developing Layer-wise theory for other types of shape or structural analysis.

In the current study, we develop an advanced mathematical framework based on Layer-wise theory. This semi-analytical framework is able accurately to predict mechanical structural responses, including the buckling load, natural frequency, deformation, and stress distributions of thick fiber-steered laminated composite conical panels. The solution is obtained for fiber-steered conical panels with arbitrary boundary conditions where this solution can be deduced for cylindrical shells and circular plates.

2 FIBER-STEERED LAMINATED COMPOSITE CONICAL PANELS

A fiber-steered laminated composite conical panel, shown in Fig. 1, is considered in the cylindrical coordinate system $(x,\ \theta,\ z)$ located on the mid-surface and mid-span of the laminate where x, θ, and z are the axial, circumferential, and radial coordinates, respectively. The composite conical panel dimensions are presented as length L, total thickness h, minor reference radius R_b, semi-vertex angle α, and span (or revolving) angle $2\theta_0$. It is worth noting that from the conical panel both the cylindrical shell for $\alpha = 0$, and the circular plate for $\alpha = \pi/2$ can be deduced.

2.1. Fiber-Steering Paths for VS Conical Panels

In this study, we consider two different path definitions. The first is a path with a linear angle variation, and the second is a path with constant curvature, which simplifies evaluation of a curvature constraint that may be imposed because of machine limitations [28].

2.1.1. Path with Linearly Varying Fiber Angles

The fiber angle on a conical panel is defined to vary linearly along the axial direction from T_0 at the small radius to T_1 at the large radius [28]:

$$\varphi(x) = T_0 + (T_1 - T_0)\frac{x}{L} \tag{1}$$

where $\varphi(x)$ is fiber orientation along the fiber path.

2.1.2. Constant Curvature Path

A path with constant curvature is also defined (see Fig. 2) so that the curvature constraint can be readily evaluated. Again, starting from an angle T_0 at R_b and ending at an angle T_1 at R_1, the angle variation is according to [28]:

$$\varphi(x) = \arcsin\left(\frac{R_b \sin T_0}{R_0(x)} + \frac{\kappa}{\sin\alpha}\left(\frac{R_0(x)^2 - R_b^2}{2R_0(x)}\right)\right) \tag{2a}$$

The corresponding value of the curvature is:

$$\kappa = \frac{1}{L}\left(\frac{2R_1}{R_1 + R_b}\sin T_1 - \frac{2R_b}{R_1 + R_b}\sin T_0\right) \tag{2b}$$

The standard notation to define a particular VS laminate with these fiber path definitions is represented by $<T_0|T_1>$, for a single layer, where $T_0 = T_1$ represents a straight fiber. The shifting direction of the reference fiber path, affecting both fiber angle and defect distribution, plays a major role in the maximum performance that can be achieved by fiber-steering [17].

3 DISPLACEMENT FIELD

In LWT, the displacement components of a generic point in the laminate are assumed as [1]:

$$u(x,\theta,z,t)=U_k\,(x,\theta,t)\Phi_k(z) \tag{3a}$$
$$v(x,\theta,z,t)=V_k\,(x,\theta,t)\Phi_k(z) \tag{3b}$$
$$w(x,\theta,z,t)=W_k\,(x,\theta,t)\Phi_k(z) \qquad (k=1,2,...,N+1) \tag{3c}$$

where k, here and in what follows, being a dummy index implies summation of terms from k=1 to k=N+1. In Eqs. (3a-c), u (x, θ, z, t), v (x, θ, z, t), and w (x, θ, z, t) denote the displacement components in the x, θ, and z directions, respectively. U_k (x, θ, t), V_k (x, θ, t), and W_k (x, θ, t) also represent the displacements of the points initially located on the kth surface of variable stiffness composite conical panels in the x, θ, and z directions, respectively, as seen in Fig. 1. Moreover, Φ_k (z) is the global Lagrangian interpolation function used for the discretization of the displacement through-thickness. The strain-displacement relations are given as:

$$\begin{gathered}
\varepsilon_{xx}=U_{k,x}\Phi_k, \qquad \varepsilon_{\theta\theta}=\frac{R_\theta}{R_0\left(R_\theta+z\right)}\left(V_{k,\theta}\Phi_k+U_k\Phi_k\sin\alpha+W_k\Phi_k\cos\alpha\right), \\
\varepsilon_{zz}=W_k\Phi'_k, \qquad \gamma_{x\theta}=V_{k,x}\Phi_k+\frac{R_\theta}{R_0\left(R_\theta+z\right)}\left(U_{k,\theta}\Phi_k-V_k\Phi_k\sin\alpha\right), \\
\gamma_{xz}=W_{k,x}\Phi_k+U_k\Phi'_k, \qquad \gamma_{\theta z}=V_k\Phi'_k+\frac{R_\theta}{R_0\left(R_\theta+z\right)}\left(W_{k,\theta}\Phi_k-V_k\Phi_k\sin\alpha\right)
\end{gathered} \tag{4}$$

where $R_\theta=\frac{R_0}{\cos\alpha}$ and $R_0=R_b+x\sin\alpha$. In Eq. (4) and what follows, a prime indicates an ordinary differentiation with respect to a z variable.

4 EQUATIONS OF MOTION

The equilibrium equations of a thick fiber-steered laminated composite conical panel with N numerical layers can be obtained using the principle of virtual displacement as follows:

$$\int_{t_1}^{t_2}\left(\delta U+\delta V-\delta K\right)dt=0 \tag{5}$$

where δU, δV, and δK are the virtual strain energy, virtual work done by external forces, and virtual kinetic energy, respectively. Employing the fundamental lemma of calculus of variations, the equilibrium equations of variable stiffness composite conical panels are obtained as:

$$\begin{aligned}
\delta U_k:\quad & Q_x^k R_0+R_x^k\cos\alpha+N_\theta^k\sin\alpha-\frac{\partial Q_{x\theta}^k}{\partial\theta}-\frac{\partial M_x^k}{\partial x}\cos\alpha-\frac{\partial N_x^k}{\partial x}R_0=\frac{2T_0}{R_0+z_k}\left(R_0+z_k\cos\alpha\right)\sin\theta \\
& +\frac{2M_0}{R_0+z_k}\left(R_0+z_k\cos\alpha\right)+2F_0\left(R_0+z_k\cos\alpha\right)-R_0 I^{kj}\ddot{U}_j
\end{aligned} \tag{6a}$$

$$\begin{aligned}
\delta V_k:\quad & Q_\theta^k R_0+R_{\theta z}^k\cos\alpha-Q_{\theta z}^k\sin\alpha-Q_{x\theta}^k\sin\alpha-\frac{\partial R_{x\theta}^k}{\partial x}\cos\alpha-\frac{\partial Q_{x\theta}^k}{\partial x}R_0-\frac{\partial N_\theta^k}{\partial\theta} \\
& =\frac{2T_0}{R_0+z_k}\left(R_0+z_k\cos\alpha\right)\cos\theta-R_0 I^{kj}\ddot{V}_j
\end{aligned} \tag{6b}$$

$$\begin{aligned}
\delta W_k:\quad & N_\theta^k\cos\alpha+N_z^k R_0+M_z^k\cos\alpha-\frac{\partial R_z^k}{\partial x}\cos\alpha-\frac{\partial Q_z^k}{\partial x}R_0-\frac{\partial Q_{\theta z}^k}{\partial\theta} \\
& -\left(R_0+z_k\cos\alpha\right)q\left(x,\theta,t\right)\delta_{k(N+1)}-\left(R_0+z_k\cos\alpha\right)\hat{N}_{xx}^k W_{k,xx} \\
& -\frac{1}{R_0}\left(1+\frac{z_k}{R_\theta}\right)\hat{N}_{\theta\theta}^k W_{k,\theta\theta}-2\left(1+\frac{z_k}{R_\theta}\right)\hat{N}_{x\theta}^k W_{k,x\theta}=-R_0 I^{kj}\ddot{W}_j
\end{aligned} \tag{6c}$$

$$\left(k=1,2,...,N+1\right)$$

where δ_{kj} is the Kronecker delta. The intensity of the applied external transverse force is denoted by q (x, θ, t) and ρ (x, θ, z) represents the conical panel density, and mass terms I^{kj} are defined as:

$$\mathrm{I}^{kj} = \int_{-h/2}^{h/2} \rho \Phi_k \Phi_j \left(1+\frac{z}{R_\theta}\right) dz \tag{7}$$

Eqs. (6) are, in general, 3(N+1) equilibrium equations corresponding to 3(N+1) unknown functions U_k, V_k, and W_k. The generalized stress and moment resultants are defined as:

$$\left(N_x^k, N_\theta^k, Q_{x\theta}^k, Q_{\theta z}^k, Q_z^k\right) = \int_{-h/2}^{h/2} \left(\sigma_{xx}, \sigma_{\theta\theta}, \tau_{x\theta}, \tau_{\theta z}, \tau_{xz}\right) \Phi_k \, dz \tag{8a}$$

$$\left(M_x^k, R_{x\theta}^k, R_z^k\right) = \int_{-h/2}^{h/2} \left(\sigma_{xx}, \tau_{x\theta}, \tau_{xz}\right) z \Phi_k \, dz \tag{8b}$$

$$\left(N_z^k, Q_x^k, Q_\theta^k\right) = \int_{-h/2}^{h/2} \left(\sigma_{zz}, \tau_{xz}, \tau_{\theta z}\right) \Phi_k' \, dz \tag{8c}$$

$$\left(M_z^k, R_x^k, R_{\theta z}^k\right) = \int_{-h/2}^{h/2} \left(\sigma_{zz}, \tau_{xz}, \tau_{\theta z}\right) z \Phi_k' \, dz \tag{8d}$$

It is noted that in Eqs. (7) and (8), the superscript k refers to the kth layer in the variable stiffness composite cylinder.

5 SPACE SOLUTION

In this section, we introduce a numerical methodology for solving the coupled governing differential equations (16) in the spatial coordinate system for alternative boundary conditions of the fiber-steered composite conical panels, i.e. simply-supported, clamped, and free boundary conditions. The Galerkin method is adopted here for solving the governing differential equations. Mathematical expressions for boundary conditions considered in this study are presented as [1]:

(a) Immovable simply-supported edges (S):

$$\begin{aligned} &U_k = V_k = W_k = 0 \qquad \text{at} \qquad x = 0, L \\ &U_k = V_k = W_k = 0 \qquad \text{at} \qquad \theta = \pm\theta_0 \end{aligned} \tag{9a}$$

(b) Clamped edges (C):

$$\begin{aligned} &U_k = V_k = W_k = \frac{\partial W_k}{\partial \theta} = \frac{\partial W_k}{\partial x} = 0 \qquad \text{at} \qquad x = 0, L \\ &U_k = V_k = W_k = \frac{\partial W_k}{\partial \theta} = \frac{\partial W_k}{\partial x} = 0 \qquad \text{at} \qquad \theta = \pm\theta_0 \end{aligned} \tag{9b}$$

(c) Free edges (F):

$$\begin{aligned} &N_x^k = M_x^k = Q_{x\theta}^k = R_{x\theta}^k = R_z^k = 0 \qquad \text{at} \qquad x = 0, L \\ &N_\theta^k = Q_{\theta z}^k = Q_{x\theta}^k = R_{x\theta}^k = R_z^k = 0 \qquad \text{at} \qquad \theta = \pm\theta_0 \end{aligned} \tag{9c}$$

where k = 1, 2, …, N+1. To implement the Galerkin method, the displacement field should be expressed in the following form for the arbitrary boundary conditions [1]:

$$\begin{aligned} &U_k(x,\theta,t) = \sum_{m=1}^{\infty}\sum_{n=1}^{\infty} U_k^{mn}(t) \frac{\partial \Phi_m(x)}{\partial x} \Phi_n(\theta) \\ &V_k(x,\theta,t) = \sum_{m=1}^{\infty}\sum_{n=1}^{\infty} V_k^{mn}(t) \Phi_m(x) \frac{\partial \Phi_n(\theta)}{\partial \theta} \\ &W_k(x,\theta,t) = \sum_{m=1}^{\infty}\sum_{n=1}^{\infty} W_k^{mn}(t) \Phi_m(x) \Phi_n(\theta) \qquad (k = 1, 2, ..., N+1) \end{aligned} \tag{10}$$

where U_k^{mn}, V_k^{mn}, and W_k^{mn} are unknown coefficients that should be determined to satisfy the governing equations, with m and n as arbitrary integers for summation; and

$$\Phi_m(x) = \alpha_1 \cosh(\lambda_m x) + \alpha_2 \cos(\lambda_m x) - \zeta_m \left(\alpha_3 \sinh(\lambda_m x) + \alpha_4 \sin(\lambda_m x)\right)$$
$$\Phi_n(\theta) = \beta_1 \cosh(\lambda_n \theta) + \beta_2 \cos(\lambda_n \theta) - \zeta_n \left(\beta_3 \sinh(\lambda_n \theta) + \beta_4 \sin(\lambda_n \theta)\right) \tag{11}$$

where λ_m and λ_n are defined in Table 1 for alternative boundary conditions. Using the Galerkin method and the approximate displacement field (Eq. (10)), and Eq. (11), we can solve the governing differential equations [1]:

$$\int_{-\theta_0}^{\theta_0}\int_0^L \left\{ \begin{array}{c} R_1\left(U_k^{mn}, V_k^{mn}, W_k^{mn}\right) \dfrac{\partial \Phi_p(x)}{\partial x} \Phi_q(\theta) \\ R_2\left(U_k^{mn}, V_k^{mn}, W_k^{mn}\right) \Phi_p(x) \dfrac{\partial \Phi_q(\theta)}{\partial \theta} \\ R_3\left(U_k^{mn}, V_k^{mn}, W_k^{mn}\right) \Phi_p(x) \Phi_q(\theta) \end{array} \right\} dx d\theta = 0 \tag{12}$$

$$\left(p = 1, 2, ..., \text{ and } q = 1, 2, ...\right)$$

where R_i (i = 1, 2, and 3) are the residuals of the governing differential equations for the admissible displacement field (Eq. (10)). Substituting Eq. (10) in governing equations and then applying the Galerkin formulation (Eq. (12)) leads to an expanded formulation, which yields a system of 3(N+1) differential equations as follows:

$$\begin{bmatrix} M_{11} & [0]_{(N+1)\times(N+1)} & [0]_{(N+1)\times(N+1)} \\ [0]_{(N+1)\times(N+1)} & M_{22} & [0]_{(N+1)\times(N+1)} \\ [0]_{(N+1)\times(N+1)} & [0]_{(N+1)\times(N+1)} & M_{33} \end{bmatrix} \begin{Bmatrix} \ddot{U}_k^{mn} \\ \ddot{V}_k^{mn} \\ \ddot{W}_k^{mn} \end{Bmatrix} + \begin{bmatrix} K_{11} & K_{12} & K_{13} \\ K_{21} & K_{22} & K_{23} \\ K_{31} & K_{32} & K_{33} + \hat{N} \end{bmatrix} \begin{Bmatrix} U_k^{mn} \\ V_k^{mn} \\ W_k^{mn} \end{Bmatrix}$$
$$= \left\{ \begin{array}{c} \dfrac{2T_{mn}}{R_0 + z_k}\left(R_0 + z_k \cos\alpha\right)\sin\theta + \dfrac{2M_{mn}}{R_0 + z_k}\left(R_0 + z_k \cos\alpha\right) + 2F_{mn}\left(R_0 + z_k \cos\alpha\right) \\ \dfrac{2T_{mn}}{R_0 + z_k}\left(R_0 + z_k \cos\alpha\right)\cos\theta \\ \left(R_0 + z_k \cos\alpha\right) Q_{mn} \delta_{k(N+1)} \end{array} \right\} \tag{13}$$

It should be observed that [M] and [K] are symmetric stiffness and mass matrices, respectively, and their components can be obtained by integration of [M'] and [K'], using Eq. (12). In addition, $\widehat{N}$ is a function of buckling loads for alternative boundary conditions. For harmonic and free vibration analyses, solutions in the following form are sought for Eq. (13):

$$U_k^{mn}(t) = U_k^{mn0} e^{i\omega_{mn}t}, \qquad V_k^{mn}(t) = V_k^{mn0} e^{i\omega_{mn}t}, \qquad W_k^{mn}(t) = W_k^{mn0} e^{i\omega_{mn}t} \tag{14}$$

Substitution of Eq. (14) in Eq. (13) yields an eigenvalue problem in the absence of mechanical load and nonlinear in-plane force resultant $\widehat{N}$. The fundamental frequency of the panels can be obtained by solving the following eigenvalue problem:

$$\left|[K] - \omega^2 [M]\right| = 0 \tag{15}$$

where ω is the fundamental frequency of the FG panel and |...| represent determinant in Eq. (15). The smallest eigenvalue obtained from Eq. (15) is called the fundamental vibration frequency. It should be noted that the nonlinear displacement term $\widehat{N}$ is omitted for static bending and forced vibration analysis, but it is preserved for the bifurcation buckling study of fiber-steered composite conical panels. Admissible trigonometric functions for different boundary conditions of fiber-steered composite conical panels are presented in Table 1, in which the symbols S, C, and F stand for immovable simply-supported, clamped and free edges, respectively. For example, CSCS refers to a fiber-steered composite conical panel with clamped edges at x = 0 and L and simply-supported edges at $\theta = \pm\theta_0$. It should be mentioned that admissible functions must satisfy the essential boundary conditions (i.e., generalized displacement) of the problem.

6 RESULTS AND DISCUSSION

The mechanical analysis of thin to thick fiber-steered composite conical panels is performed. Two paths for fiber-steering are considered including a path with a linear angle variation, and a path with constant curvature. A uniformly distributed transverse load is considered to obtain the deflection and stress. All physical layers are assumed to have equal thickness (= 0.125 mm [10]) and are modeled as being made up of p numerical layers. In all the subsequent calculations, p is set equal to 9. The material properties of composites used for the analysis of constant and variable stiffness laminates are given in Table 2 [5]. We consider a conical panel made of a 40-ply balanced and symmetric laminate with a variable stiffness design of $[\pm\langle T_0|T_1\rangle]_{10s}$ with the length L= 10.777 cm (L/h = 21.5), minor reference radius R_b = 6 cm, semi-vertex angle $\alpha = 21.80°$, and span angle $2\theta_0$ = 90° [10] (unless otherwise mentioned). The out-of-plane deflection (w), critical buckling load (N_{cr}), fundamental frequency (ω), and stress (σ) are given in the following non-dimensional form:

$$\bar{w} = w_0 \frac{E_{22}h^3}{L^4 q_0}, \quad \bar{N} = N_{cr}\frac{L^2}{E_{22}h^3}, \qquad \bar{\omega} = \omega\frac{L^2}{h}\sqrt{\frac{\rho}{E_{22}}}, \qquad \bar{\sigma} = \frac{\sigma}{q_0} \quad (16)$$

6.1. *Effects of Geometrical Parameters on Mechanical Response*

In this section, we study the effects of boundary conditions, number of layers, and geometrical parameters, such as length L, semi-vertex angle α, and span angle $2\theta_0$, of conical panels on the mechanical responses of constant curvature fiber-steered conical panels with the lay-up sequences of $[\pm\langle 0|90\rangle]_{10s}$.

Figure 2 illustrates a design chart for fiber-steered composite conical panels with the $[\pm\langle 0|90\rangle]_{10s}$ lay-up sequence with a constant curvature path *for* the non-dimensional critical buckling load× maximum deflection ($\bar{\boldsymbol{N}}\,\bar{\boldsymbol{w}}_{\boldsymbol{max}}$) versus the non-dimensional fundamental frequency× maximum deflection ($\bar{\boldsymbol{\omega}}\,\bar{\boldsymbol{w}}_{\boldsymbol{max}}$) for different boundary conditions presented in Table 1 including CCCC, SSSS, CCFF, and SSFF in Fig. 2a; and CSCS, CCSS, CFCF, and SFSF in Fig. 2b. Semi-vertex angle increases from α = 0° to α = 90°, and the length increases from L = $0.5R_b$ to L = $2.5R_b$. As can be seen in Fig. 2, the effectiveness of a variable stiffness laminate depends on the boundary conditions. For example, a CCCC boundary condition shifts the buckling load-frequency domain to be higher.

7 CONCLUSION

We develop a semi-analytical methodology to accurately predict the mechanical responses of thick fiber-steered composite conical panels. The model enables modelling and analysis of fiber-steered panels in the form of conical shells, cylindrical shells, and circular plates. Static bending, tension, torsion, buckling, and free vibration analyses have been formulated. We have first presented the governing equations obtained via Layer-wise theory, and then solved them by using the hybrid Fourier-Galerkin method.

Table 1: Values of α_j, λ_i, and ζ_i for S-S, C-C, F-F, C-S, C-F and F-S boundary conditions [1].

Boundary conditions	α_j or β_j (j=1, 2, 3, and 4)	Characteristic equations and values of $\mu\lambda_i$ ($L\times\lambda_m$ or $2\theta_0\times\lambda_n$)	ζ_i (ζ_m or ζ_n)
S-S	α_1=0, α_2=0 α_3=0, α_4=-1	$\sin(\mu\lambda_i)=0$ mπ or nπ	1 or 1
C-C	α_1=1, α_2=-1 α_3=1, α_4=-1	$\cos(\mu\lambda_i)\cosh(\mu\lambda_i)=1$ $\mu\lambda_i$=4.730, 7.853, …	$\frac{\cosh(\mu\lambda_i)-\cos(\mu\lambda_i)}{\sinh(\mu\lambda_i)-\sin(\mu\lambda_i)}$
F-F	α_1=-1, α_2=-1 α_3=-1, α_4=-1	$\cos(\mu\lambda_i)\cosh(\mu\lambda_i)=1$ $\mu\lambda_i$=4.730, 7.853, …	$\frac{\cosh(\mu\lambda_i)-\cos(\mu\lambda_i)}{\sinh(\mu\lambda_i)-\sin(\mu\lambda_i)}$

C-S	α_1=1, α_2=-1 α_3=1, α_4=-1	tan($\mu\lambda_i$)=tanh($\mu\lambda_i$) $\mu\lambda_i$=3.927, 7.069, …	$\dfrac{\cosh(\mu\lambda_i)-\cos(\mu\lambda_i)}{\sinh(\mu\lambda_i)-\sin(\mu\lambda_i)}$
C-F	α_1=1, α_2=-1 α_3=1, α_4=-1	cos($\mu\lambda_i$)cosh($\mu\lambda_i$)=-1 $\mu\lambda_i$=1.875, 4.694, …	$\dfrac{\cosh(\mu\lambda_i)+\cos(\mu\lambda_i)}{\sinh(\mu\lambda_i)+\sin(\mu\lambda_i)}$
F-S	α_1=1, α_2=1 α_3=1, α_4=1	tan($\mu\lambda_i$)=tanh($\mu\lambda_i$) $\mu\lambda_i$=3.927, 7.069, …	$\dfrac{\cosh(\mu\lambda_i)-\cos(\mu\lambda_i)}{\sinh(\mu\lambda_i)-\sin(\mu\lambda_i)}$

Table 2: Material properties of the composite laminates [23, 41].

Mechanical properties	Value
E_{11}	143 (GPa)
E_{22}=E_{33}	9.1 (GPa)
G_{12}	4.82 (GPa)
G_{13}= G_{23}	4.9 (GPa)
υ_{12}=υ_{13}=υ_{23}	0.3
ρ	1500 (kg/m^3)

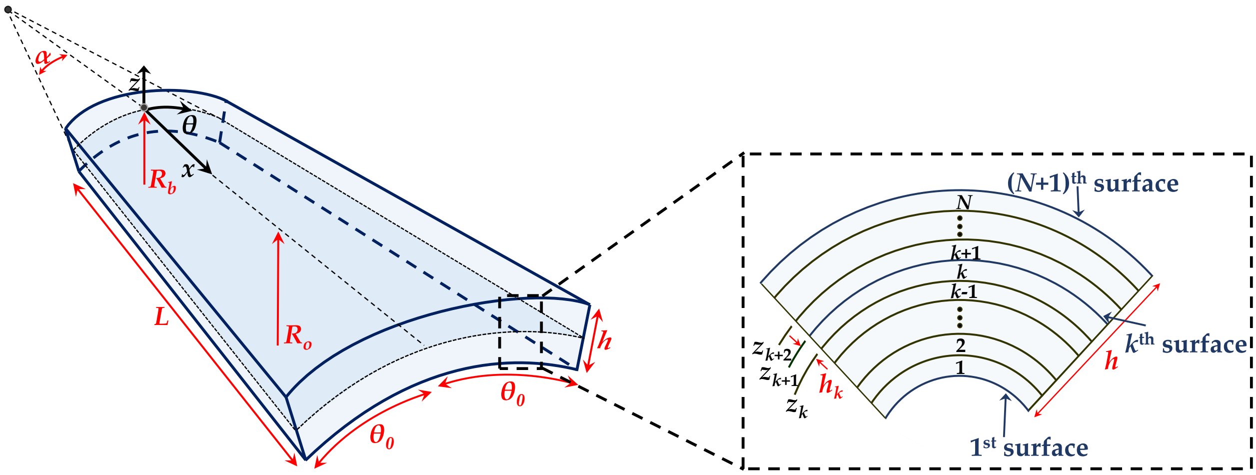

Figure 1: Geometry of an *N*-layered fiber-steered composite conical panel: the coordinate system, ply sequences.

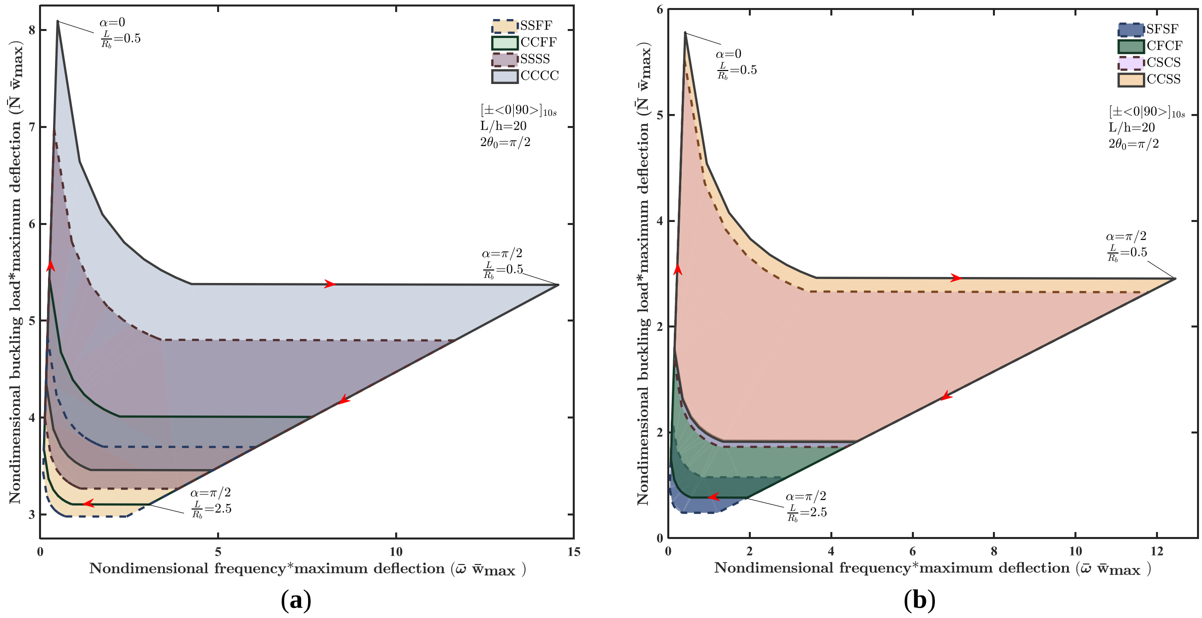

Figure 2: Design chart for fiber-steered composite conical panels $[\pm<0|90>]_{10s}$ with a constant curvature path for the non-dimensional critical buckling load×maximum deflection ($\bar{\boldsymbol{N}}\,\bar{\boldsymbol{w}}_{\boldsymbol{max}}$) vs. the non-dimensional fundamental frequency×maximum deflection ($\bar{\boldsymbol{\omega}}\,\bar{\boldsymbol{w}}_{\boldsymbol{max}}$).

8 REFERENCES

[1] Reddy JN. Mechanics of laminated composite plates and shells: theory and analysis. CRC press 2004.

[2] Hyer MW, Charette RF. Use of curvilinear fiber format in composite structure design. AIAA Journal 1991;29(6):1011-5.

[3] Gürdal Z, Olmedo R. In-plane response of laminates with spatially varying fiber orientations: variable stiffness concept. AIAA Journal 1993;31(4):751-8.

[4] Sabido A, Bahamonde L, Harik R, van Tooren MJ. Maturity assessment of the laminate variable stiffness design process. Composite Structures 2017;160:804-12.

[5] Blom AW, Stickler PB, Gürdal Z. Optimization of a composite cylinder under bending by tailoring stiffness properties in circumferential direction. Composites Part B: Engineering 2010;41(2):157-65.

[6] Rouhi M, Ghayoor H, Hoa SV, Hojjati M. Effect of structural parameters on design of variable-stiffness composite cylinders made by fiber steering. Composite Structures 2014;118:472-81.

[7] Goldfeld Y, Arbocz J. Buckling of laminated conical shells given the variations of the stiffness coefficients. AIAA Journal 2004;42(3):642-9.

[8] Sun M, Hyer MW. Use of material tailoring to improve buckling capacity of elliptical composite cylinders. AIAA Journal 2008;46(3):770-82.

[9] Wu CP, Lee CY. Differential quadrature solution for the free vibration analysis of laminated conical shells with variable stiffness. Int Journal of Mechanical Sciences 2001;43(8):1853-69.

[10] Blom AW, Setoodeh S, Hol JM, Gürdal Z. Design of variable-stiffness conical shells for maximum fundamental eigenfrequency. Computers & Structures 2008;86(9):870-8.

[11] Wu K, Gurdal Z. Thermal testing of tow-placed, variable stiffness panels. 19th AIAA Applied Aerodynamics Conference 2001:1190.

[12] Abdalla MM, Gürdal Z, Abdelal GF. Thermomechanical response of variable stiffness composite panels. Journal of Thermal Stresses 2008;32(1-2):187-208.

[13] White SC, Weaver PM, Wu KC. Post-buckling analyses of variable-stiffness composite cylinders in axial compression. Composite Structures 2015;123:190-203.

[14] Ungwattanapanit T, Kamath S, Baier H. Gradient-Based Optimization of Postbuckled, Steered-Fiber Aircraft Shell Using Equivalent Static Loads. 57th AIAA/ASCE/AHS/ASC Structures, Structural Dynamics, and Materials Conference 2016:1967.
[15] Toropov VV, Jones R, Willment T, Funnell M. Weight and manufacturability optimization of composite aircraft components based on a genetic algorithm. 6th world congresses of structural and multidisciplinary optimization, Rio de Janeiro, Brazil. 2005 May 30;30.
[16] Blom AW, Lopes CS, Kromwijk PJ, Gurdal Z, Camanho PP. A theoretical model to study the influence of tow-drop areas on the stiffness and strength of variable-stiffness laminates. Journal of Composite Materials 2009;43(5):403-425.
[17] Akbarzadeh AH, Nik MA, Pasini D. The role of shear deformation in laminated plates with curvilinear fiber paths and embedded defects. Composite Structures 2014;118:217-27.
[18] Akbarzadeh AH, Nik MA, Pasini D. Vibration responses and suppression of variable stiffness laminates with optimally steered fibers and magnetostrictive layers. Composites Part B: Engineering 2016;91:315-26.
[19] Tullu A, Kang BS. Elastic deformation of fiber-reinforced multi-layered composite cylindrical shells of variable stiffness. Composites Part B: Engineering 2016;100:44-55.
[20] Tullu A, Ku TW, Kang BS. Elastic deformation of fiber-reinforced multi-layered composite conical shell of variable stiffness. Composite Structures 2016;154:634-45.
[21] Sarvestani HY, Sarvestani MY. Interlaminar stress analysis of general composite laminates. Int Journal of Mechanical Sciences 2011;53(11):958-67.
[22] Sarvestani HY, Sarvestani MY. Free-edge stress analysis of general composite laminates under extension, torsion and bending. Applied Mathematical Modelling 2012;36(4):1570-88.
[23] Sarvestani HY, Hojjati M. Failure analysis of thick composite curved tubes. Composite Structures 2017;160:1027-41.
[24] Sarvestani HY, Hojjati M. Three-dimensional stress analysis of orthotropic curved tubes-part 2: laminate solution. European Journal of Mechanics-A/Solids 2016;60:339-58.
[25] Yazdani S, Ribeiro P, Rodrigues JD. A p-version layerwise model for large deflection of composite plates with curvilinear fibres. Composite Structures 2014;108:181-90.
[26] Houmat A. Nonlinear free vibration of laminated composite rectangular plates with curvilinear fibers. Composite Structures 2013;106:211-24.
[27] Tornabene F, Fantuzzi N, Bacciocchi M. Higher-order structural theories for the static analysis of doubly-curved laminated composite panels reinforced by curvilinear fibers. Thin-Walled Structures 2016;102:222-45.
[28] Blom AW. Structural performance of fiber-placed, variable-stiffness composite conical and cylindrical shells. Delft University of Technology 2010.